

TIFR/TH/03-04

Higgs and SUSY Searches at LHC: An Overview

D.P. Roy

Tata Institute of Fundamental Research,
Homi Bhabha Road, Mumbai 400 005, India

I start with a brief summary of Higgs mechanism and supersymmetry. Then I discuss the theoretical constraints, current limits and search strategies for Higgs boson(s) at LHC — first in the SM and then in the MSSM. Finally I discuss the analogous constraints and search strategies for the superparticles, concentrating on the minimal supergravity model. Recent advances in identifying the most promising channels for Higgs and SUSY searches are emphasised.

As per the Standard Model (SM) the basic constituents of matter are the quarks and leptons, which interact by the exchange of gauge bosons – photon, gluon and the massive W and Z bosons. By now we have seen all the quarks and leptons as well as the gauge bosons. But the story is not complete yet because of the mass and the hierarchy problems.

Mass Problem (Higgs Mechanism):

The problem is how to give mass to the weak gauge bosons, W and Z , without breaking gauge symmetry, which is required for a renormalisable field theory. In order to appreciate it consider the weak interaction Lagrangian of a charged scalar field ϕ ; i.e.

$$\mathcal{L} = \left(\partial_\mu \phi + ig \frac{\vec{\tau}}{2} \vec{W}_\mu \phi \right)^\dagger \left(\partial_\mu \phi + ig \frac{\vec{\tau}}{2} \vec{W}_\mu \phi \right) - \left[\mu^2 \phi^\dagger \phi + \lambda (\phi^\dagger \phi)^2 \right] - \frac{1}{4} \vec{W}_{\mu\nu} \vec{W}_{\mu\nu}, \quad (1)$$

where

$$\vec{W}_{\mu\nu} = \partial_\mu \vec{W}_\nu - \partial_\nu \vec{W}_\mu - g \vec{W}_\mu \times \vec{W}_\nu \quad (2)$$

is the field tensor for the weak gauge bosons \vec{W}_μ . The charged and the neutral W bosons form a $SU(2)$ vector, reflecting the nonabelian nature of this gauge group. This is responsible for the last term in (2), which leads to gauge boson self-interaction. Correspondingly the gauge transformation on \vec{W}_μ has an extra term, i.e.

$$\phi \rightarrow e^{i\vec{\alpha} \cdot \vec{\tau}} \phi, \quad \vec{W}_\mu \rightarrow \vec{W}_\mu - \frac{1}{g} \partial_\mu \vec{\alpha} - \vec{\alpha} \times \vec{W}_\mu. \quad (3)$$

This ensures gauge invariance of $\vec{W}_{\mu\nu}$, and hence for the last term of the Lagrangian, representing gauge kinetic energy. Evidently the middle term, representing scalar mass and self-interaction, is invariant under gauge transformation on ϕ . Finally the first term, representing scalar kinetic energy and gauge interaction, can be easily shown to be invariant under the simultaneous gauge transformations (3). However the addition of a mass term

$$-M^2 \vec{W}_\mu \cdot \vec{W}_\mu, \quad (4)$$

would clearly break the gauge invariance of the Lagrangian. Note that, in contrast the scalar mass term, $\mu^2 \phi^\dagger \phi$, is clearly gauge invariant. This phenomenon is exploited to give mass to the gauge bosons through back door

without breaking the gauge invariance of the Lagrangian. This is the celebrated Higgs mechanism of spontaneous symmetry breaking [1].

One starts with a $SU(2)$ doublet of complex scalar field ϕ with imaginary mass, i.e. $\mu^2 < 0$. Consequently the minimum of the scalar potential, $\mu^2\phi^\dagger\phi + \lambda(\phi^\dagger\phi)^2$, moves out from the origin to a finite value

$$v = \sqrt{-\mu^2/\lambda}, \quad (5)$$

i.e. the field develops a finite vacuum expectation value. Since the perturbative expansion in quantum field theory is stable only around a local minimum, one has to translate the field by the constant quantity,

$$\phi^o = v + H^o(x), \quad (6)$$

where the superscript denotes the electric charge. Thus one gets a valid perturbative field theory in terms of the redefined field H . This represents the physical Higgs boson, while the 3 other components of the complex doublet field are absorbed to give mass and hence longitudinal components to the gauge bosons.

Substituting (6) in the first term of the Lagrangian (1) leads to a mass term for W ,

$$M_W = \frac{1}{2}gv. \quad (7)$$

It also leads to a HWW coupling,

$$\frac{1}{2}g^2v = gM_W, \quad (8)$$

i.e. the Higgs coupling to the gauge bosons is proportional to the gauge boson mass. Similarly its couplings to quarks and leptons can be shown to be proportional to their respective masses, i.e.

$$h_{\ell,q} = m_{\ell,q}/v = \frac{1}{2}gm_{\ell,q}/M_W. \quad (9)$$

Indeed, this is the source of the fermion masses in the SM. Finally substituting (6) in the middle term of the Lagrangian leads to a real mass for the physical Higgs boson,

$$M_H = v\sqrt{2\lambda} = M_W(2\sqrt{2\lambda}/g). \quad (10)$$

Substituting $M_W = 80$ GeV and $g = 0.65$ along with a perturbative limit on the scalar self-coupling $\lambda \lesssim 1$, implies that the Higgs boson mass is bounded by $M_H < 1000$ GeV. But the story does not end here. Giving mass to the gauge bosons via the Higgs mechanism leads to the so called hierarchy problem.

Hierarchy Problem (Supersymmetry):

The problem is how to control the Higgs scalar mass in the desired range of a few hundred GeV. This is because the scalar masses are known to have quadratically divergent quantum corrections from radiative loops. These would push the output scalar mass to the cut-off scale of the SM, i.e. the GUT scale (10^{16} GeV) or the Planck scale (10^{19} GeV). The desired mass range of $\sim 10^2$ GeV is clearly tiny compared to these scales. This is the so called hierarchy problem. The underlying reason for the quadratic divergence is that the scalar masses are not protected by any symmetry unlike the fermion and the gauge boson masses, which are protected by chiral symmetry and gauge symmetry. Of course it was this very property of the scalar mass that was exploited to give masses to the fermions and gauge bosons in the first place. The hierarchy problem is the flip side of the same coin.

The most attractive solution to this problem is provided by supersymmetry (SUSY), a symmetry between fermions and bosons [2]. It predicts the quarks and leptons to have scalar superpartners called squarks and sleptons ($\tilde{q}, \tilde{\ell}$), and the gauge bosons to have fermionic superpartners called gauginos ($\tilde{g}, \tilde{\gamma}, \tilde{W}, \tilde{Z}$). In the minimal supersymmetric extension of the standard model (MSSM) one needs two Higgs doublets $H_{1,2}$, with opposite hypercharge $Y = \pm 1$, to give masses to the up and down type quarks. The corresponding fermionic superpartners are called Higgsinos ($\tilde{H}_{1,2}$). The opposite hypercharge of these two sets of fermions ensures anomaly cancellation.

SUSY ensures that the quadratically divergent quantum corrections from quark, lepton and Higgs boson loops are cancelled by the contributions from the corresponding squark, slepton and Higgsino loops. Thus the Higgs masses can be kept in the desired range of $\sim 10^2$ GeV. However this implies two important constraints on SUSY breaking.

- i) SUSY can be broken in masses but not in couplings (soft breaking), so that the co-efficients of the cancelling contributions remain equal and opposite.

- ii) The size of SUSY breaking in masses is $\sim 10^2$ GeV, so that the size of the remainder remains within this range. Thus the superpartners of the SM particles are also expected to lie in the mass range of $\sim 10^2$ GeV, going upto 1000 GeV.

SM Higgs Boson: Theoretical Constraints & Search Strategy

The Higgs self coupling λ is ultra-violet divergent. It evolves according to the renormalisation group equation (RGE)

$$\frac{d\lambda}{d\ln(Q/M_W)} = \frac{3\lambda^2}{2\pi^2}. \quad (11)$$

It can be easily solved to give

$$\lambda(Q) = \frac{1}{1/\lambda(M_W) - (3/2\pi^2)\ln(Q/M_W)}, \quad (12)$$

which has a Landau pole at

$$Q_0 = M_W e^{2\pi^2/3\lambda(M_W)}, \quad \lambda(M_W) = \frac{g^2}{8} \frac{M_H^2}{M_W^2}. \quad (13)$$

Thus the larger the starting value $\lambda(M_W)$, the sooner will the coupling diverge. Evidently the theory is valid only upto a cut-off scale $\Lambda = Q_0$. Requiring the theory to be valid at all energies, $\Lambda \rightarrow \infty$, would imply $\lambda(M_W) \rightarrow 0$; i.e. the only good $\lambda\phi^4$ theory is a trivial theory. Surely we do not want that. But if we want the theory to be valid upto the Planck scale or GUT scale, we must have a relatively small $\lambda(M_W)$, which corresponds to a small $M_H \lesssim 200$ GeV. If on the other hand we assume it to be valid only upto the TeV scale, then we can have a larger $\lambda(M_W)$, corresponding to a relatively large $M_H \lesssim 600$ GeV. This is the so-called triviality bound [3]. If M_H is significantly larger than 600 GeV, then the range of validity of the theory is limited to $\Lambda < 2M_H$. This would correspond to a composite Higgs scenario, e.g. technicolour models.

Fig. 1 shows the triviality bound on the Higgs mass against the cut-off scale Λ of the theory [4]. It also shows a lower bound on the Higgs mass,

which comes from a negative contribution to the RGE (11) from the top Yukawa coupling, i.e.

$$\frac{d\lambda}{d\ln(Q/M_W)} = \frac{3}{2\pi^2}(\lambda^2 + \lambda h_t^2 - h_t^4). \quad (14)$$

The Yukawa coupling being ultra-violet divergent turns λ negative at a high energy scale; and the smaller the starting value of λ (or equivalently M_H) the sooner will it become negative. A negative λ coupling has the undesirable feature of an unstable vacuum. Thus one can define a cut-off scale Λ for the theory, where this change of sign occurs. The lower curve of Fig. 1 shows the lower bound on M_H as a function of the cut-off scale Λ including the theoretical uncertainty [5]. We see from this figure that the longer the range of validity of the theory, the stronger will be the upper and lower bounds on M_H . Thus assuming no new physics upto the GUT or Planck scale (the desert scenario) would constrain the SM Higgs mass to lie in the range

$$M_H = 130 - 180 \text{ GeV}. \quad (15)$$

However the lower bound becomes invalid once we have more than one Higgs doublet, since the unique relation between the top mass and Yukawa coupling (9) will no longer hold. In particular, one expects an upper bound of ~ 130 GeV for the lightest Higgs boson mass in MSSM instead of a lower bound, as we shall see below. Since one needs SUSY or some other form of new physics to stabilize the Higgs mass, the above vacuum stability bound may have limited significance. Nonetheless it is interesting to note that the predicted range of the SM Higgs boson mass (15) agrees favourably with the indirect estimate of this quantity from the precision measurement of electro-weak parameters at LEP/SLD [6], i.e.

$$M_H = 88_{-37}^{+60} \text{ GeV } (< 206 \text{ GeV at 95\% CL}). \quad (16)$$

The search strategy for Higgs boson is based on its preferential coupling to the heavy quarks and gauge bosons as seen from (8,9). The LEP-I search was based on the so called Bjorken process

$$e^+e^- \rightarrow Z \rightarrow HZ^* \rightarrow \bar{b}b(\ell^+\ell^-, \nu\nu, \bar{q}q), \quad (17)$$

while the LEP-II search is based on the associated process with Z and Z^* intercharged, resulting in the limit [7]

$$M_H > 114.1 \text{ GeV}. \quad (18)$$

Thus a promising mass range to probe for the SM Higgs boson signals is

$$M_H = 114 - 206 \text{ GeV}. \quad (19)$$

But the upper limit is not a robust one since the underlying quantum corrections have only logarithmic dependence on the Higgs mass. Fig. 2 shows the total decay width of the Higgs boson along with the branching ratios for the important decay channels [8]. It is clear from this figure that the mass range can be divided into two parts – a) $M_H < 2M_W$ (90–160 GeV) and b) $M_H > 2M_W$ (160–1000 GeV).

The first part is the so called intermediate mass region, where the Higgs width is expected to be only a few MeV. The dominant decay mode is $H \rightarrow \bar{b}b$. This has unfortunately a huge QCD background, which is ~ 1000 times larger than the signal. By far the cleanest channel is $\gamma\gamma$, where the continuum background is a 2nd order EW process. However, it suffers from a small branching ratio

$$B(H \rightarrow \gamma\gamma) \sim 1/1000, \quad (20)$$

since it is a higher order process, induced by the W boson loop. So one needs a very high jet/ γ rejection factor $\gtrsim 10^4$. Besides the continuum background being proportional to $\Delta M_{\gamma\gamma}$, one needs a high resolution,

$$\Delta M_{\gamma\gamma} \lesssim 1 \text{ GeV} \text{ i.e. } \lesssim 1\% \text{ of } M_H. \quad (21)$$

This requires fine EM calorimetry, capable of measuring the γ energy and direction to 1% accuracy.

One can get a feel for the size of the signal from the Higgs production cross-sections shown in Fig. 3. The relevant production processes are

$$gg \xrightarrow{\bar{t}^* t^*} H, \quad (22)$$

$$qq \xrightarrow{W^* W^*} Hqq, \quad (23)$$

$$q\bar{q}' \xrightarrow{W^*} HW, \quad (24)$$

$$gg, q\bar{q} \rightarrow Ht\bar{t}(Hb\bar{b}). \quad (25)$$

The largest cross-section, coming from gluon-gluon fusion via the top quark loop (22), is of the order of $10 pb$ in the intermediate mass region. Thus the expected size of the $H \rightarrow \gamma\gamma$ signal is $\sim 10 fb$, corresponding to $\sim 10^3$ events

at the high luminosity ($\sim 100 \text{ fb}^{-1}$) run of LHC. The estimated continuum background is $\sim 10^4$ events, which can of course be subtracted out. Thus the significance of the signal is given by its relative size with respect to the statistical uncertainty in the background, i.e.

$$S/\sqrt{B} \simeq 10. \quad (26)$$

Fig. 4 shows the ATLAS (left) and CMS (right) simulations for the SM Higgs signals at LHC from different decay channels. The ATLAS figure shows the expected significance level of the signal for the high luminosity (100 fb^{-1}) run of LHC. Combining the different decay channels should give a $\geq 10\sigma$ signal over the entire Higgs mass range of 100 - 1000 GeV. The CMS figure shows the minimum luminosity required for the discovery of a 5σ Higgs signal against its mass. It shows that a modest luminosity of $\sim 20 \text{ fb}^{-1}$, which is expected to be accumulated at the low luminosity run, should suffice for this discovery over most of Higgs mass range of interest.

As we see from Fig. 4, the most promising Higgs decay channel is

$$H \rightarrow ZZ \rightarrow \ell^+ \ell^- \ell^+ \ell^-, \quad (27)$$

since reconstruction of the $\ell^+ \ell^-$ invariant masses makes it practically background free. Thus it provides the most important Higgs signal right from the subthreshold region of $M_H = 140 \text{ GeV}$ upto 600 GeV. Note however a sharp dip in the ZZ branching ratio at $M_H = 160 - 170 \text{ GeV}$ due to the opening of the WW channel (see Fig. 2). The most important Higgs signal in this dip region is expected to come from [10]

$$H \rightarrow WW \rightarrow \ell^+ \nu \ell^- \bar{\nu}. \quad (28)$$

However in general this channel suffers from a much larger background for two reasons – i) it is not possible to reconstruct the W masses because of the two neutrinos and ii) there is a large WW background from $t\bar{t}$ decay.

For large Higgs mass, $M_H = 600 - 1000 \text{ GeV}$, the 4-lepton signal (27) becomes too small in size. In this case the decay channels

$$H \rightarrow WW \rightarrow \ell \nu q \bar{q}', \quad H \rightarrow ZZ \rightarrow \ell^+ \ell^- \nu \nu \quad (29)$$

are expected to provide more favourable signals. The biggest background comes from single $W(Z)$ production along with QCD jets. However, one can

exploit the fact that a large part of the signal cross-section in this case comes from WW fusion (23), which is accompanied by two forward (large-rapidity) jets. One can use the double forward jet tagging to effectively control the background. Indeed the above simulation studies by the CMS and ATLAS collaborations show that using this strategy one can extend the Higgs search right upto 1000 GeV [9].

MSSM Higgs Bosons: Theoretical Constraints & Search Strategy

As mentioned earlier, the MSSM contains two Higgs doublets, which correspond to 8 independent states. After 3 of them are absorbed by the W and Z bosons, one is left with 5 physical states: two neutral scalars h^0 and H^0 , a pseudoscalar A^0 , and a pair of charged Higgs scalars H^\pm . At the tree-level their masses and couplings are determined by only two parameters – the ratio of the two vacuum expectation values, $\tan \beta$, and one of the scalar masses, usually taken to be M_A . However, the neutral scalars get a large radiative correction from the top quark loop along with the top squark (stop) loop. To a good approximation this is given by [11]

$$\epsilon = \frac{3g^2 m_t^4}{8\pi^2 M_W^2} \ln \left(\frac{M_{\tilde{t}}^2}{m_t^2} \right), \quad (30)$$

plus an additional contribution from the $\tilde{t}_{L,R}$ mixing,

$$\epsilon_{\text{mix}} = \frac{3g^2 m_t^4}{8\pi^2 M_W^2} \frac{A_t^2}{M_{\tilde{t}}^2} \left(1 - \frac{A_t^2}{12 M_{\tilde{t}}^2} \right) \leq \frac{9g^2 m_t^4}{8\pi^2 M_W^2}. \quad (31)$$

Thus while the size of ϵ_{mix} depends on the trilinear SUSY breaking parameter A_t , it has a definite maximum value. As expected the radiative corrections vanish in the exact SUSY limit. One can estimate the rough magnitude of these corrections assuming a SUSY breaking scale of $M_{\tilde{t}} = 1$ TeV. The leading log QCD corrections can be taken into account by using the running mass of top at the appropriate energy scale [11]; i.e. $m_t(\sqrt{m_t M_{\tilde{t}}}) \simeq 157$ GeV in (30) and $m_t(M_{\tilde{t}}) \simeq 150$ GeV in (31) instead of the top pole mass of 175 GeV. One can easily check the resulting size of the radiative corrections are

$$\epsilon \sim M_W^2 \quad \text{and} \quad 0 < \epsilon_{\text{mix}} \lesssim M_W^2. \quad (32)$$

The neutral scalar masses are obtained by diagonalising the mass-squared matrix

$$\begin{pmatrix} M_A^2 \sin^2 \beta + M_Z^2 \cos^2 \beta & -(M_A^2 + M_Z^2) \sin \beta \cos \beta \\ -(M_A^2 + M_Z^2) \sin \beta \cos \beta & M_A^2 \cos^2 \beta + M_Z^2 \sin^2 \beta + \epsilon' \end{pmatrix} \quad (33)$$

with $\epsilon' = (\epsilon + \epsilon_{\text{mix}})/\sin^2 \beta$. Thus

$$\begin{aligned} M_h^2 &= \frac{1}{2} \left[M_A^2 + M_Z^2 + \epsilon' - \left\{ (M_A^2 + M_Z^2 + \epsilon')^2 - 4M_A^2 M_Z^2 \cos^2 \beta \right. \right. \\ &\quad \left. \left. - 4\epsilon' (M_A^2 \sin^2 \beta + M_Z^2 \cos^2 \beta) \right\}^{1/2} \right] \\ M_H^2 &= M_A^2 + M_Z^2 + \epsilon' - M_h^2 \\ M_{H^\pm}^2 &= M_A^2 + M_W^2 \end{aligned} \quad (34)$$

where h denotes the lighter neutral scalar [12]. One can easily check that its mass has an asymptotic limit for $M_A \gg M_Z$, i.e.

$$M_h^2 \longrightarrow M_Z^2 \cos^2 2\beta + \epsilon + \epsilon_{\text{mix}}, \quad (35)$$

while $M_H^2, M_{H^\pm}^2 \rightarrow M_A^2$. Thus the MSSM contains at least one light Higgs boson h , whose tree-level mass limit $M_h < M_Z$, goes upto 130 GeV after including the radiative corrections.

Let us consider now the couplings of the MSSM Higgs bosons. A convenient parameter for this purpose is the mixing angle α between the neutral scalars, i.e.

$$\tan 2\alpha = \tan 2\beta \frac{M_A^2 + M_Z^2}{M_A^2 - M_Z^2 + \epsilon'/\cos 2\beta}, \quad -\pi/2 < \alpha < 0. \quad (36)$$

Note that

$$\alpha \xrightarrow{M_A \gg M_Z} \beta - \pi/2. \quad (37)$$

Table-I. Important couplings of the MSSM Higgs bosons h , H and A relative to those of the SM Higgs boson

Channel	H_{SM}	h	H	A
$\bar{b}b(\tau^+\tau^-)$	$\frac{gm_b}{2M_W}(m_\tau)$	$-\sin\alpha/\cos\beta$ $\rightarrow 1$	$\cos\alpha/\cos\beta$ $\tan\beta$	$\tan\beta$ ”
$\bar{t}t$	$g\frac{m_t}{2M_W}$	$\cos\alpha/\sin\beta$ $\rightarrow 1$	$\sin\alpha/\sin\beta$ $\cot\beta$	$\cot\beta$ ”
$WW(ZZ)$	$gM_W(M_Z)$	$\sin(\beta - \alpha)$ $\rightarrow 1$	$\cos(\beta - \alpha)$ 0	0 ”

Table-I shows the important couplings of the neutral Higgs bosons relative to those of the SM Higgs boson. The limiting values of these couplings at large M_A are indicated by arrows. The corresponding couplings of the charged Higgs boson, which has no SM analogue, are

$$\begin{aligned}
 H^+\bar{t}b &: \frac{g}{\sqrt{2}M_W}(m_t \cot\beta + m_b \tan\beta), \quad H^+\tau\nu : \frac{g}{\sqrt{2}M_W}m_\tau \tan\beta, \\
 H^+W^-Z &: 0.
 \end{aligned} \tag{38}$$

Note that the top Yukawa coupling is ultraviolet divergent. Assuming it to lie within the perturbation theory limit all the way upto the GUT scale implies

$$1 < \tan\beta < m_t/m_b, \tag{39}$$

which is therefore the favoured range of $\tan\beta$. However, it assumes no new physics beyond the MSSM upto the GUT scale, which is a stronger assumption than MSSM itself. Nontheless we shall concentrate in this range.

Before discussing the search of MSSM Higgs bosons at LHC let us briefly discuss the LEP constraints on these particles. Fig. 5 plots the h^0 , H^0 and

H^\pm masses against M_A for two representative values of $\tan\beta$ ($= 3$ and 30) assuming maximum stop mixing [13]. It also plots the corresponding $\sin^2(\beta - \alpha)$, representing the suppression factor of the h signal relative to the SM Higgs boson for the LEP process (17). We see that for $\tan\beta = 3$, the maximum value of h mass is marginally above the SM Higgs mass limit of 114 GeV. Moreover the corresponding lower limit of M_h is marginally smaller than this value since the signal suppression factor is ≥ 0.5 . Thus $\tan\beta = 3$ lies just inside the LEP allowed region, while it disallows $\tan\beta \leq 2.4$. The disallowed region extends over $\tan\beta \lesssim 5$ for a more typical value of the mixing parameter, $A_t \simeq 1$ TeV. One also sees from this figure that the lower limit of $M_h \geq 114$ GeV will hold at large $\tan\beta$ (~ 30) if M_A is > 130 GeV. But for lower values of M_A this signal is strongly suppressed at large $\tan\beta$; and one can only get a modest limit of $M_A \simeq M_h > 90$ GeV from the pair-production process $e^+e^- \rightarrow hA$ at LEP [7]. The pair production of charged Higgs bosons at LEP gives a limit $M_{H^\pm} > 78$ GeV, which is close to its theoretical mass limit (34).

Coming back to the neutral Higgs couplings of Table-I, we see that in the large M_A limit the light Higgs boson (h) couplings approach the SM values. The other Higgs bosons are not only heavy, but their most important couplings are also suppressed. This is the so called decoupling limit, where the MSSM Higgs sector is phenomenologically indistinguishable from the SM. It follows therefore that the Higgs search strategy at LHC for $M_A \gg M_Z$ should be the same as the SM case, i.e. via

$$h \rightarrow \gamma\gamma. \quad (40)$$

At lower M_A , several of the MSSM Higgs bosons become light. Unfortunately their couplings to the most important channels, $\bar{t}t$ and WW/ZZ , are suppressed relative to the SM Higgs boson [12]. Thus their most important production cross-sections as well as their decay BRs into the $\gamma\gamma$ channel are suppressed relative to the SM case. Consequently the Higgs detection in this region is very challenging. Nonetheless recent simulation studies show that it will be possible to see at least one of the MSSM Higgs bosons at LHC over the full parameter space of M_A and $\tan\beta$. Fig. 6 shows such a simulation by the CMS collaboration [14] for integrated luminosities of 30 fb^{-1} and 100 fb^{-1} , which are expected from the low and high luminosity runs of LHC respectively. It looks much more promising now than 4-5 years back, when the

corresponding plot showed a big hole in the middle of this parameter space [15]. The improvement comes from the following three processes, which have been studied only during the last few years.

- 1) $t\bar{t}h, h \rightarrow b\bar{b}$: The $h \rightarrow b\bar{b}$ decay width is enhanced by the $\sin^2 \alpha / \cos^2 \beta$ factor, while the $h \rightarrow \gamma\gamma$ width via the W boson loop is suppressed by $\sin^2(\beta - \alpha)$ as $M_A \rightarrow M_Z$. Besides in the latter case the production cross-section via the top quark loop is suppressed by a cancelling contribution from the stop loop. Hence the above process provides a viable signature for h over the modest m_A region where the canonical $h \rightarrow \gamma\gamma$ signature becomes too small.
- 2) $tH^\pm, H^\pm \rightarrow \tau\nu(t\bar{t})$: While the earlier analyses of charged Higgs boson signal at LHC were restricted to $M_{H^\pm} < m_t$ ($M_A \lesssim 140$ GeV) [16], recently they have been extended for heavier H^\pm via these processes [17,18]. In particular the associated production of tH^\pm followed by the $H^\pm \rightarrow \tau\nu$ decay is seen to provide a viable signature over a large range of M_{H^\pm} (M_A) for $\tan \beta \gtrsim 10$. Here one exploits the predicted τ polarization, i.e. $P_\tau = +1$ for the H^\pm signal and -1 for the W^\pm background. In the 1-prong hadronic decay channel of τ , the $P_\tau = +1(-1)$ state is peaked at $R \simeq 1$ (0.4), where R denotes the fraction of the visible τ -jet momentum carried by the charged prong [18]. Following this suggestion a simple kinematic cut of $R > 0.8$ has been used in the above simulation [14] to effectively suppresses the $W^\pm \rightarrow \tau\nu$ as well as the fake τ background from QCD jets, while retaining nearly half the signal events.
- 3) $H, A \rightarrow \tau^+\tau^- \rightarrow 2\tau\text{-jets}$: Earlier analyses of this process assumed at least one of the τ 's to have leptonic decay. The above simulation shows that hadronic decay of both the taus provides a viable signature over a wider range of M_A . This signature can be improved further by exploiting the correlation between the polarizations of the 2 taus as suggested in [19].

Note that all these three new channels require identification of b quark and/or hadronic τ -jet. Thus they are based on tracker performance, while the canonical $h \rightarrow \gamma\gamma$ channel emphasised EM calorimeter.

Finally one should note from Fig. 6 that there is a large part of the parameter space, where one can see only one Higgs boson (h) with SM like couplings and hence not be able to distinguish the SUSY Higgs sector from the SM. Fortunately it will be possible to probe SUSY directly via superparticle search at LHC as we see below.

Superparticles: Signature & Search Strategy

I shall concentrate on the standard R -parity conserving SUSY model, where

$$R = (-1)^{3B+L+2S} \quad (41)$$

is defined to be $+1$ for the SM particles and -1 for their superpartners, since they differ by $1/2$ unit of spin S . It automatically ensures Lepton and Baryon number conservation by preventing single emission (absorption) of superparticle.

Thus R -conservation implies that (i) superparticles are produced in pair and (ii) the lightest superparticle (LSP) is stable. There are strong astrophysical constraints against such a stable particle carrying colour or electric charge, which imply that the LSP is either sneutrino $\tilde{\nu}$ or photino $\tilde{\gamma}$ (or in general the lightest neutralino). The latter alternative is favoured by most SUSY models. In either case the LSP is expected to have only weak interaction with ordinary matter like the neutrino, since e.g.

$$\tilde{\gamma}q \xrightarrow{\tilde{q}} q\tilde{\gamma} \quad \text{and} \quad \nu q \xrightarrow{W} eq' \quad (42)$$

have both electroweak couplings and $M_{\tilde{q}} \sim M_W$. This makes the LSP an ideal candidate for the Cold Dark Matter. It also implies that the LSP would leave the normal detectors without a trace like the neutrino. The resulting imbalance in the visible momentum constitutes the canonical missing transverse-momentum (\cancel{p}_T) signature for superparticle production at hadron colliders. It is also called the missing transverse-energy (\cancel{E}_T) as it is often measured as a vector sum of the calorimetric energy deposits in the transverse plane.

The main processes of superparticle production at LHC are the QCD processes of quark-antiquark and gluon-gluon fusion [20]

$$q\bar{q}, gg \longrightarrow \tilde{q}\bar{\tilde{q}}(\tilde{g}\tilde{g}). \quad (43)$$

The NLO corrections can increase these cross-sections by $15 - 20\%$ [21]. The simplest decay processes for the produced squarks and gluinos are

$$\tilde{q} \rightarrow q\tilde{\gamma}, \quad \tilde{g} \rightarrow q\bar{q}\tilde{\gamma}. \quad (44)$$

Convoluting these with the pair production cross-sections gave the simplest jets + \not{p}_T signature for squark/gluino production, which were adequate for the early searches for relatively light squarks and gluinos. However, over the mass range of current interest (≥ 100 GeV) the cascade decays of squark and gluino into the LSP via the heavier chargino/neutralino states are expected to dominate over the direct decays. This is both good news and bad news. On the one hand the cascade decay degrades the missing- p_T of the canonical jets + \not{p}_T signature [22]. But on the other hand it gives a new multilepton signature via the leptonic decays of these chargino/neutralino states [23]. It may be noted here that one gets a mass limit of $M_{\tilde{q},\tilde{g}} \gtrsim 200$ GeV from the Tevatron data using either of the two signatures [7].

The cascade decay is described in terms of the $SU(2) \times U(1)$ gauginos $\tilde{W}^{\pm,0}, \tilde{B}^0$ along with the Higgsinos $\tilde{H}^\pm, \tilde{H}_1^0$ and \tilde{H}_2^0 . The \tilde{B} and \tilde{W} masses are denoted by M_1 and M_2 respectively while the Higgsino masses are given by the supersymmetric mass parameter μ . The charged and the neutral gauginos will mix with the corresponding Higgsinos to give the physical chargino $\chi_{1,2}^\pm$ and neutralino $\chi_{1,2,3,4}^0$ states. Their masses and compositions can be found by diagonalising the corresponding mass matrices, i.e.

$$M_C = \begin{pmatrix} M_2 & \sqrt{2}M_W \sin \beta \\ \sqrt{2}M_W \cos \beta & \mu \end{pmatrix}, \quad (45)$$

$$M_N = \begin{pmatrix} M_1 & 0 & -M_Z \sin \theta_W \cos \beta & M_Z \sin \theta_W \sin \beta \\ 0 & M_2 & M_Z \cos \theta_W \cos \beta & -M_Z \cos \theta_W \sin \beta \\ -M_Z \sin \theta_W \cos \beta & M_Z \cos \theta_W \cos \beta & 0 & -\mu \\ M_Z \sin \theta_W \sin \beta & -M_Z \cos \theta_W \sin \beta & -\mu & 0 \end{pmatrix}. \quad (46)$$

The LEP limit [7] on the lighter chargino χ_1^\pm mass is 100 GeV, which implies

$$|\mu|, |M_2| > 100 \text{ GeV}. \quad (47)$$

The corresponding slepton mass limits are $m_{\tilde{e}} > 99$ GeV, $m_{\tilde{\mu}} > 95$ GeV and $m_{\tilde{\tau}} > 80$ GeV. The sneutrino $\tilde{\nu}$ and the lightest neutralino χ_1^0 mass limits are 45 and 40 GeV respectively. In general the cascade decay of squarks and gluinos would depend on all these masses.

SUGRA Model: To control the number of mass parameters one has to assume a supersymmetry breaking model. The simplest and most popular model is called supergravity, where SUSY is broken in a hidden sector and its effect is communicated to the observable sector via gravitational interaction. Since this interaction is colour and flavour blind, it leads to a common SUSY breaking mass for all the scalars (m_0) and another one for all the gauginos ($M_{1/2}$) near the GUT scale. This is consistent with the successful unification of the $SU(3) \times SU(2) \times U(1)$ gauge couplings at this scale [7]. Then the SUSY breaking masses evolve to low energy scales as per the Renormalisation Group Evolution formulae [24].

The gaugino masses evolve like the corresponding gauge couplings, i.e.

$$M_i(Q) = M_{1/2} \alpha_i(Q) / \alpha(M_G). \quad (48)$$

Thus at the low energy scale, $Q \sim M_W$,

$$\begin{aligned} M_2 &= M_{1/2} \alpha_2 / \alpha(M_G) \simeq 0.8 M_{1/2}, \\ M_1 &= M_2 \alpha_1 / \alpha_2 \simeq M_2 / 2, \\ M_{\tilde{g}} &= M_3 = M_2 \alpha_3 / \alpha_2 \simeq 3 M_2. \end{aligned} \quad (49)$$

Ignoring the trilinear coupling (A) terms, one can write the SUSY breaking scalar masses at low energy as

$$m_i^2 = m_0^2 + a_i m_0^2 + b_i M_{1/2}^2, \quad (50)$$

where a_i is proportional to Yukawa coupling and b_i to combination of gauge and Yukawa couplings. Of course the Yukawa couplings are significant only for H_2 and the 3rd generation squarks and sleptons. It drives the H_2 mass

square ($m_2^2 = m_{H_2}^2 + \mu^2$) negative, as required for EWSB. The EWSB condition is

$$\frac{M_Z^2}{2} = \frac{m_{H_1}^2 - m_{H_2}^2 \tan^2 \beta}{\tan^2 \beta - 1} - \mu^2, \quad (51)$$

which reduce to $-m_{H_2}^2 - \mu^2$ over the range $\tan \beta \gtrsim 5$, favoured by LEP. Substituting the evolution eq. (50) for $m_{H_{1,2}}^2$ in (51) gives [24]

$$\mu^2 \simeq m_0^2 \left(\frac{9}{7}y - 1 \right) - M_{1/2}^2 \left(0.5 - 6y + \frac{18}{7}y^2 \right) - \frac{M_Z^2}{2}, \quad (52)$$

where y denotes the top Yukawa coupling relative to its fixed point value. For the physical top mass of 175 GeV it is given by [25,26,27]

$$y = \frac{h_t^2}{h_f^2} = \frac{1 + 1/\tan^2 \beta}{1.44} \simeq 0.71, \quad (53)$$

where the last equality holds to within 2% accuracy over $\tan \beta \geq 5$. Substituting this in (52) give

$$\mu^2 \simeq -0.08m_0^2 + 2.4M_{1/2}^2 - 0.5M_Z^2. \quad (54)$$

Thus one has only two independent parameters m_0 and $M_{1/2}$ apart from $\tan \beta$ and the sign of μ . The small coefficient of the m_0^2 term in (54) along with (49) imply that over most of the parameter space $\mu^2 > M_2^2$, i.e. the lighter chargino and neutralino states are gauginos (\tilde{W}, \tilde{B}) obeying the mass hierarchy (49). However there is a narrow strip of very high m_0^2 region, where its negative contribution pushes $|\mu|$ down to the LEP limit of 100 GeV. Here the lighter chargino and neutralinos are Higgsino or mixed states. This is the focus point region of ref. [26], which is favoured by the electron and neutron EDM constraints [28]. It is also favoured by the cosmological constraint on the relic density of Dark Matter [29], as we see below.

Fig. 7 shows the contours of DM relic density in the $m_0 - M_{1/2}$ plane for a representative value of $\tan \beta = 10$ and +ve μ [30]. The latter is favoured by the indirect constraint from $b \rightarrow s\gamma$. The regions marked I and II correspond to $\mu < 100$ GeV and $m_{\tilde{\chi}_1^0} < m_{\tilde{\chi}_1^0}$ respectively. The former is excluded by the LEP constraint (47) and the latter by the requirement of a neutral LSP. The remaining area is within the discovery limit of LHC. The indicated upper limit from the muon anomalous magnetic moment data is not compelling

because of the uncertainty in the QCD contribution [31]. More importantly however even a bigger region is excluded by the cosmological constraint of DM relic density [7]

$$0.1 < \Omega h^2 < 0.3. \quad (55)$$

While the lower limit may be evaded by assuming alternative DM candidates, the upper limit is quite compelling.

The reason for the predicted over abundance of SUSY DM over most of the parameter space is that the LSP (χ_1^0) over this region is dominantly \tilde{B} , which does not couple to W or Z bosons. Thus they can pair-annihilate only via the exchange of massive superparticles like squarks or sleptons, $\tilde{B}\tilde{B} \xrightarrow{\tilde{q}(\tilde{\ell})} q\bar{q}(\ell^+\ell^-)$, which have low rates. However there are two strips adjacent to the disallowed regions I and II, which predict right DM relic densities. In the first one the LSP has a large Higgsino component, so that it can pair annihilate by Higgsino exchange $\tilde{H}^0\tilde{H}^0 \xrightarrow{\tilde{H}^0(\tilde{H}^\pm)} ZZ(W^+W^-)$ or simply by s -channel Z exchange $\tilde{H}^0\tilde{H}^0 \xrightarrow{Z} q\bar{q}$. At the boundary of the excluded region I the lighter chargino and neutralino states are dominantly Higgsinos, \tilde{H}^\pm and $\tilde{H}_{1,2}^0$, with nearly degenerate mass $\simeq \mu$. Thus there is also a large co-annihilation rate via s -channel W exchange $\tilde{H}^0\tilde{H}^\pm \xrightarrow{W^\pm} q'\bar{q}$. This leads to underabundance of SUSY DM ($\Omega h^2 < 0.1$) at this boundary. In the second region the $\tilde{\tau}_1$ mass is close to that of the LSP (\tilde{B}). Thus one has a fairly large pair-annihilation rate via $\tilde{\tau}_1$ exchange, resulting in the desired relic density (52). There is also co-annihilation of $\tilde{\tau}_1$ with \tilde{B} via s -channel τ at the boundary. Similar features hold at other values of $\tan\beta$ as well as negative μ [31].

Thus there is a good deal of current interest in the LHC signature of superparticles in these two strips, corresponding to i) $m_0 \gg M_{1/2}$ and ii) $m_0 \ll M_{1/2}$.

- i) This corresponds to the above mentioned focus point region. A distinctive feature of this region is an inverted mass hierarchy, where the top squarks ($\tilde{t}_{1,2}$) are predicted to be significantly lighter than those of 1st two generations. This is because $\tilde{t}_{L,R}$ have large negative Yukawa coupling contributions (a_i) in eq. (50), while the 1st two generation squark masses are $\simeq m_0$. Thus for $m_0 = 2000$ GeV, $M_{1/2} = 500$ GeV

and $\tan \beta = 10$ one predicts [27]

$$M_{\tilde{g}} \simeq 1300 \text{ GeV}, \ m_{\tilde{t}_1} \simeq 1500 \text{ GeV}, \ m_{\tilde{u}, \tilde{d}} \geq 2200 \text{ GeV}. \quad (56)$$

Consequently one predicts a large branching fraction for gluino decay via \tilde{t}_1 , i.e.

$$\tilde{g} \xrightarrow{\tilde{t}_1} \bar{t}t\tilde{\chi}_i^0, \ \bar{t}b\chi_j^\pm \rightarrow 2b2W\chi_1^0 \dots \quad (57)$$

The corresponding final state from gluino pair production contains 4*b* and 4*W* particles. Fig. 8 shows the resulting signal in single lepton, dilepton, same-sign dilepton and trilepton channels along with 4*b* tags [27]. The background is effectively suppressed by a 100 GeV cut on the accompanying H_T . The large multiplicity of *b*-quarks and *W* bosons makes this a far more spectacular signal compared to the standard cascade decade case.

- ii) In this region the \tilde{t}_1 mass is close that of $\tilde{\chi}_1^0$. Consequently there is a large branching fraction of cascade decay via \tilde{t}_1 into

$$\tilde{t}_1 \rightarrow \tau\chi_1^0. \quad (58)$$

Thus the final state contains two τ 's along with a large H_T . In this case the most promising signature corresponds to 1-prong hadronic decay of the τ 's [32]. A remarkable prediction of the SUGRA model is the polarization of τ coming from the \tilde{t}_1 decay (58). Fig. 9 shows that $P_\tau > 0.9$ over the full $m_0 - M_{1/2}$ plane at $\tan \beta = 30$, which holds at other values of $\tan \beta$ as well [33]. Moreover $P_\tau > 0.95$ in the relevant half-plane of $m_0 < M_{1/2}$. In contrast the SM background from *W* and *Z* decays correspond to $P_\tau = -1$ and 0 respectively. Fig. 10 shows the *R* distributions for $P_\tau = +1, 0, -1$. As in the case of H^\pm signal discussed earlier, one can also sharpen the SUSY signal by demanding $R > 0.8$ – i.e. the charged prong to carry $> 80\%$ of the visible τ -jet momentum.

Note that the SUSY signals in the above two regions are based on identification of *b* and hadronic τ -jets. Thus they again emphasize the tracker performance like the MSSM Higgs signals discussed earlier.

I thank the organizers of the XV DAE Symposium on High Energy Physics at Jammu University and in particular Dr. Anju Bhasin for a wonderful meeting.

References:

1. For a review see e.g. J.F. Gunion, H.E. Haber, G. Kane and S. Dawson, *The Higgs Hunters' Guide* (Addison-Wesley, Reading, MA, 1990).
2. For a review see e.g. H.E. Haber and G. Kane, *Phys. Rep.* 117, 75 (1985).
3. L. Maiani, G. Parisi and R. Petronzio, *Nucl. Phys.* B136, 115 (1978); N. Cabibbo, L. Maiani, G. Parisi and R. Petronzio, *Nucl. Phys.* B158, 295 (1979); M. Lindner, *Z. Phys.* C31, 295 (1986).
4. T. Hambye and K. Riesselmann, *Phys. Rev.* D55, 7255 (1997).
5. G. Altarelli and G. Isidori, *Phys. Lett.* B337, 141 (1994); J.A. Casas, J.R. Espinosa and M. Quiros, *Phys. Lett.* B342, 171 (1995) and B382, 374 (1996).
6. LEP and SLC Electroweak Working Group, hep-ex/0112021.
7. Review of Particle Properties: K. Hagiwara et al, *Phys. Rev.* D66, 010001 (2002).
8. M. Spira, *Fortsch. Phys.* 46, 203 (1998).
9. ATLAS Collaboration: Technical Design Report, CERN/LHCC/99-15 (1999); CMS Collaboration: M. Dittmar, *Pramana* 55, 151 (2000); D. Dittmar and A.S. Nicollerat, CMS-NOTE 2001/036.
10. M. Dittmar and H. Dreiner, *Phys. Rev.* D55, 167 (1997).
11. For a review of radiative correction along with reference to the earlier works see H.E. Haber, R. Hempfling and A.H. Hoang, *Z. Phys.* C75, 539 (1997).
12. See e.g. A. Djouadi, J. Kalinowski and P.M. Zerwas, *Z. Phys.* C70, 435 (1996).
13. A. Djouadi [hep-ph/0205248].
14. D. Denegri et al, CMS NOTE 2001/032 [hep-ph/0112045].

15. D.P. Roy, *Pramana* 51, 7 (1998) [hep-ph/9803421], see Fig. 7.
16. D.P. Roy, *Phys. Lett.* B277, 183 (1992) and *Phys. Lett.* B283, 403 (1992); S. Raychaudhuri and D.P. Roy, *Phys. Rev.* D53, 4902 (1996).
17. S. Moretti and D.P. Roy, *Phys. Lett.* B470, 209 (1999); D. Miller, S. Moretti, D.P. Roy and W. Sterling, *Phys. Rev.* D61, 055011 (2000).
18. D.P. Roy, *Phys. Lett.* B459, 607 (1999).
19. S. Moretti and D.P. Roy, *Phys. Lett.* B545, 329 (2002).
20. G.L. Kane and J.P. Levile, *Phys. Lett.* B112, 227 (1982); P.R. Harrison and C.H. Llewellyn-Smith, *Nucl. Phys.* B213, 223 (1983) [Err. *Nucl. Phys.* B223, 542 (1983)]; E. Reya and D.P. Roy, *Phys. Lett.* B141, 442 (1984); *Phys. Rev.* D32, 645 (1985).
21. W. Beenakker, R. Hopker, M. Spira and P. Zerwas, *Nucl. Phys.* B492, 51 (1997); M. Kramer, T. Plehn, M. Spira and P. Zerwas, *Phys. Rev. Lett.* 79, 341 (1997).
22. H. Baer, C. Chen, F. Paige and X. Tata, *Phys. Rev.* D52, 2746 (1995).
23. M. Guchait and D.P. Roy, *Phys. Rev.* D52, 133 (1995).
24. See e.g. M. Carena, M. Olechowski, S. Pokorski and C.E.M. Wagner, *Nucl. Phys.* B426, 269 (1994).
25. J. Bagger, K. Matchev, D. Pierce and R. Zhang, *Nucl. Phys.* B491, 3 (1997).
26. J.L. Feng, K.T. Matchev and T. Moroi, *Phys. Rev. Lett.* 84, 2322 (2000); *Phys. Rev.* D61, 075005 (2000).
27. Utpal Chattopadhyay, Amitava Datta, Anindya Datta, Aseshkrishna Datta and D.P. Roy, *Phys. Lett.* B493, 127 (2000).
28. U. Chattopadhyay, T. Ibrahim and D.P. Roy, *Phys. Rev.* D64, 013004 (2001).
29. J.L. Feng, K.T. Matchev and F. Wilczek, *Phys. Rev. Lett.* 84, 2322 (2000); *Phys. Rev.* D63, 045024 (2001).

30. U. Chattopadhyay (private communication).
31. See e.g. U. Chattopadhyay and Pran Nath [hep-ph/0208012], J.R. Ellis, A. Ferstl and K. Olive, Phys. Lett. B532, 318 (2002); H. Baer et al. [hep-ph/0210441].
32. H. Baer, C.H. Chen, M. Drees, F. Paige and X. Tata, Phys. Rev. D59, 055014 (1999); I. Hinchliffe and F. Paige, Phys. Rev. D61, 095011 (2000).
33. M. Guchait and D.P. Roy, Phys. Lett. B541, 356 (2002).

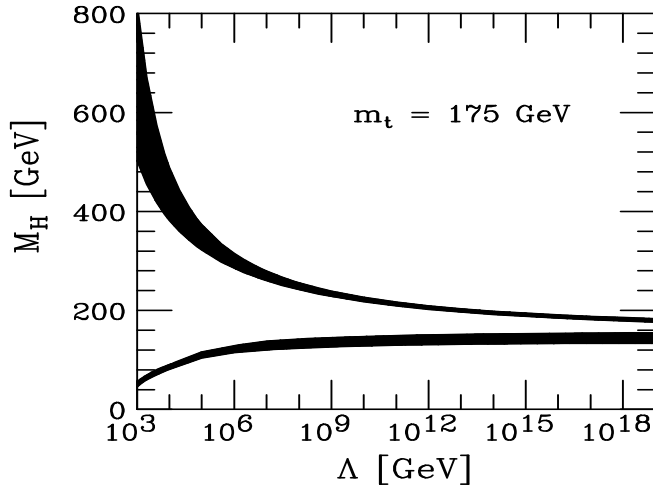


Figure 1. The upper and lower bounds on the mass of the SM Higgs boson as functions of the cutoff scale [4].

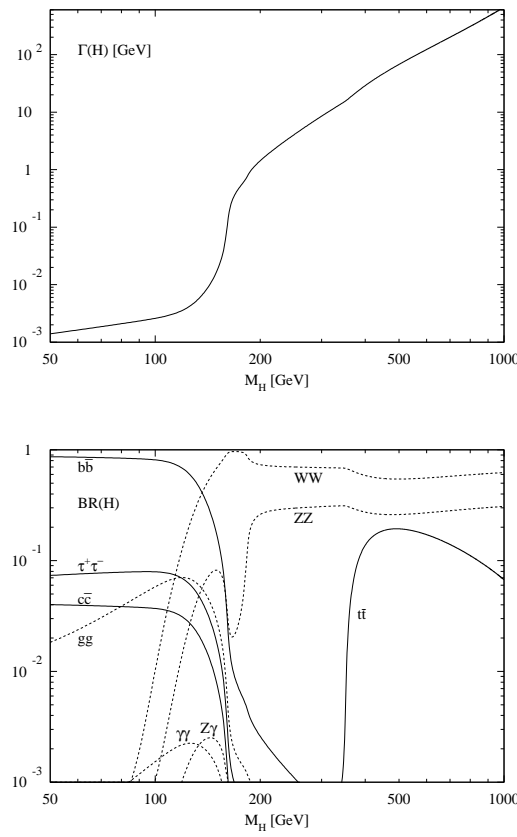


Figure 2. Total decay width and the main branching ratios of the SM Higgs boson [8].

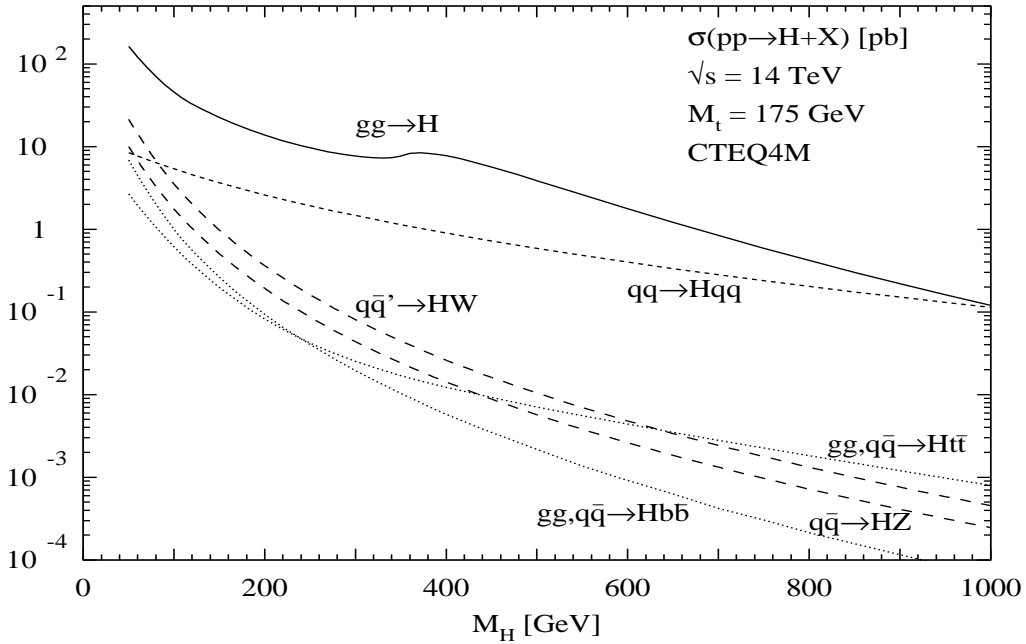


Figure 3. Production cross-sections of the SM Higgs boson at LHC [8].

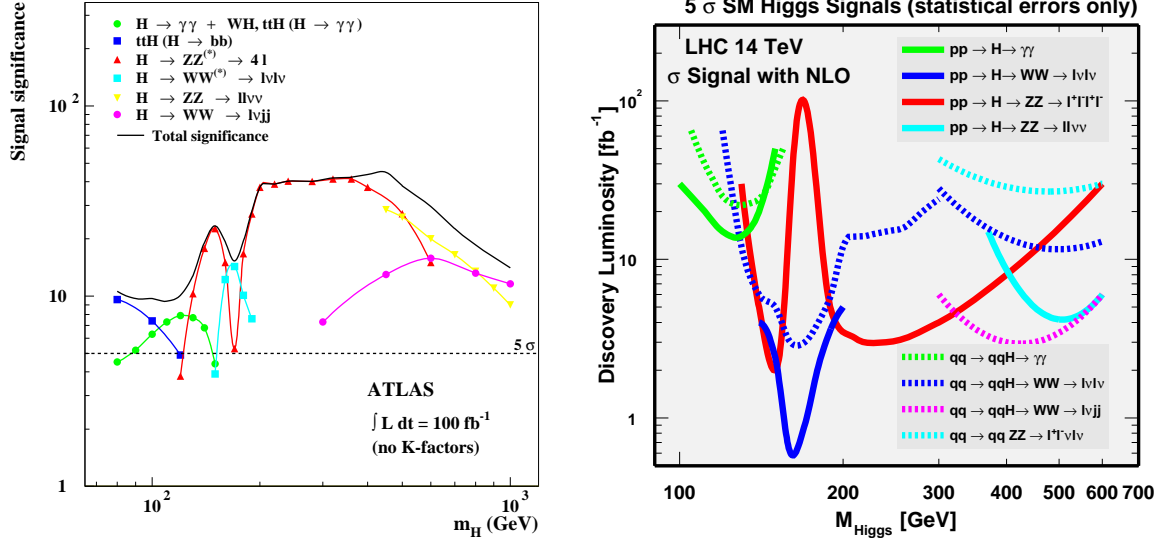


Fig. 4. (a) Significance level of the SM Higgs signal at LHC with a Luminosity of 100 fb^{-1} ; (b) Required luminosity for a 5σ Higgs signal at LHC. The first and the second figures are from the simulations of the ATLAS and CMS collaborations respectively [9].

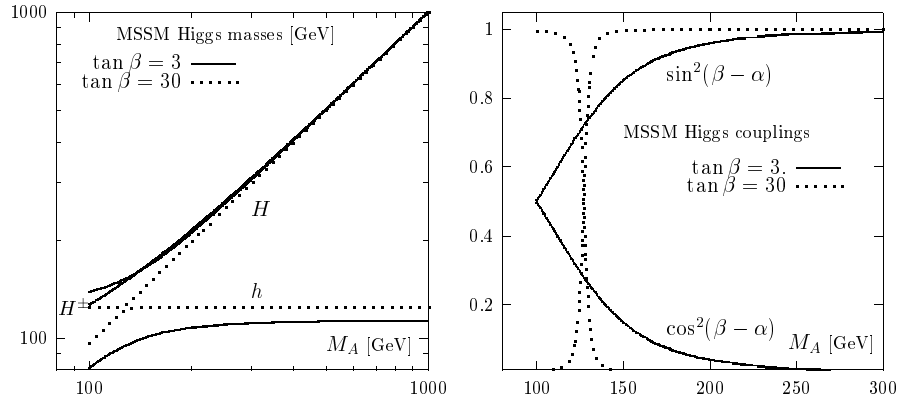


Fig. 5. Masses of the MSSM Higgs bosons and their squared couplings to WW , ZZ (relative to the SM Higgs coupling) for two representative values of $\tan \beta = 3$ and 30 , assuming maximal stop mixing [13].

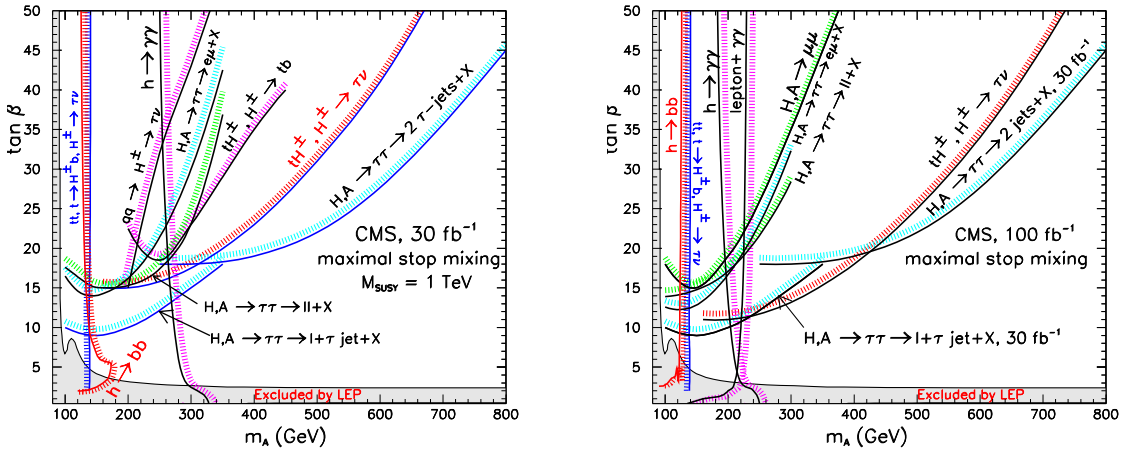


Fig. 6. Expected 5σ discovery limits of various MSSM Higgs signals at LHC for luminosities of 30 fb^{-1} and 100 fb^{-1} [14].

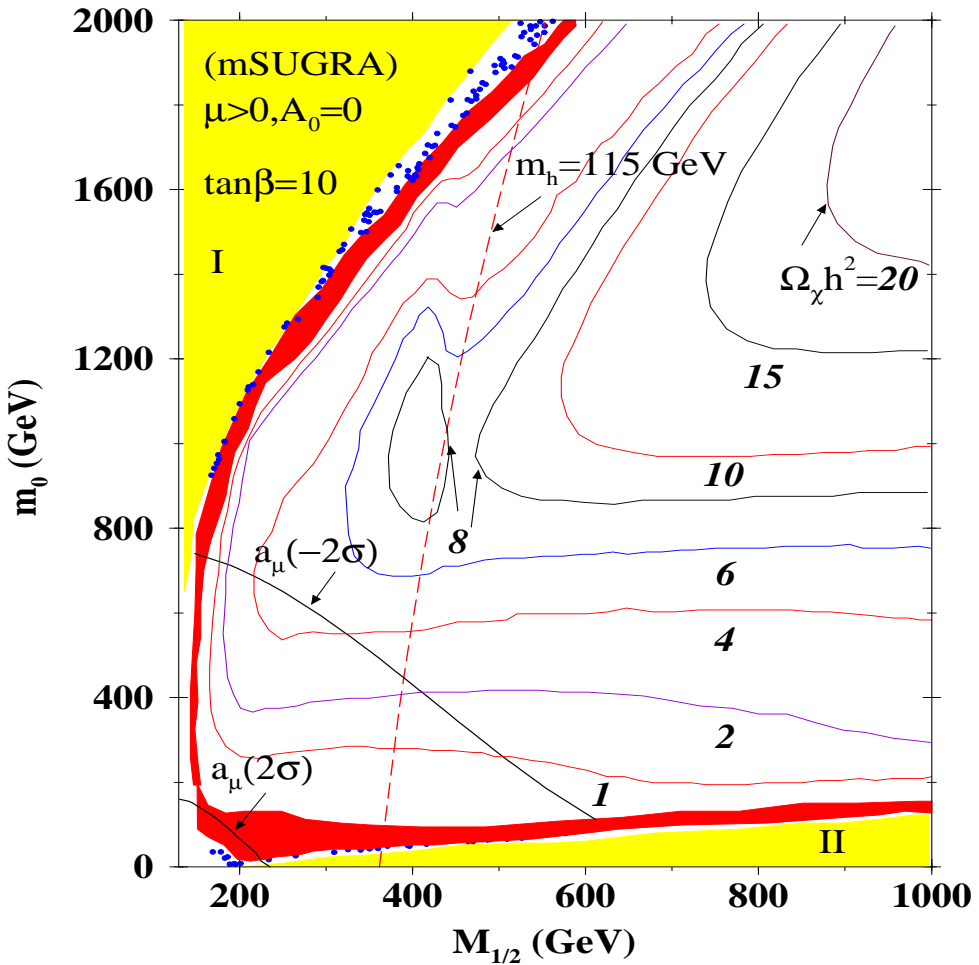


Fig. 7. Contours of DM relic density in the $m_0 - M_{1/2}$ plane for $\tan\beta = 10$ and +ve μ [30]. The excluded regions I and II correspond to $\mu < 100$ GeV and $m_{\tilde{\tau}_1} < m_{\tilde{\chi}_1^0}$ respectively. Also shown are the exclusion limits from the putative muon anomalous magnetic moment.

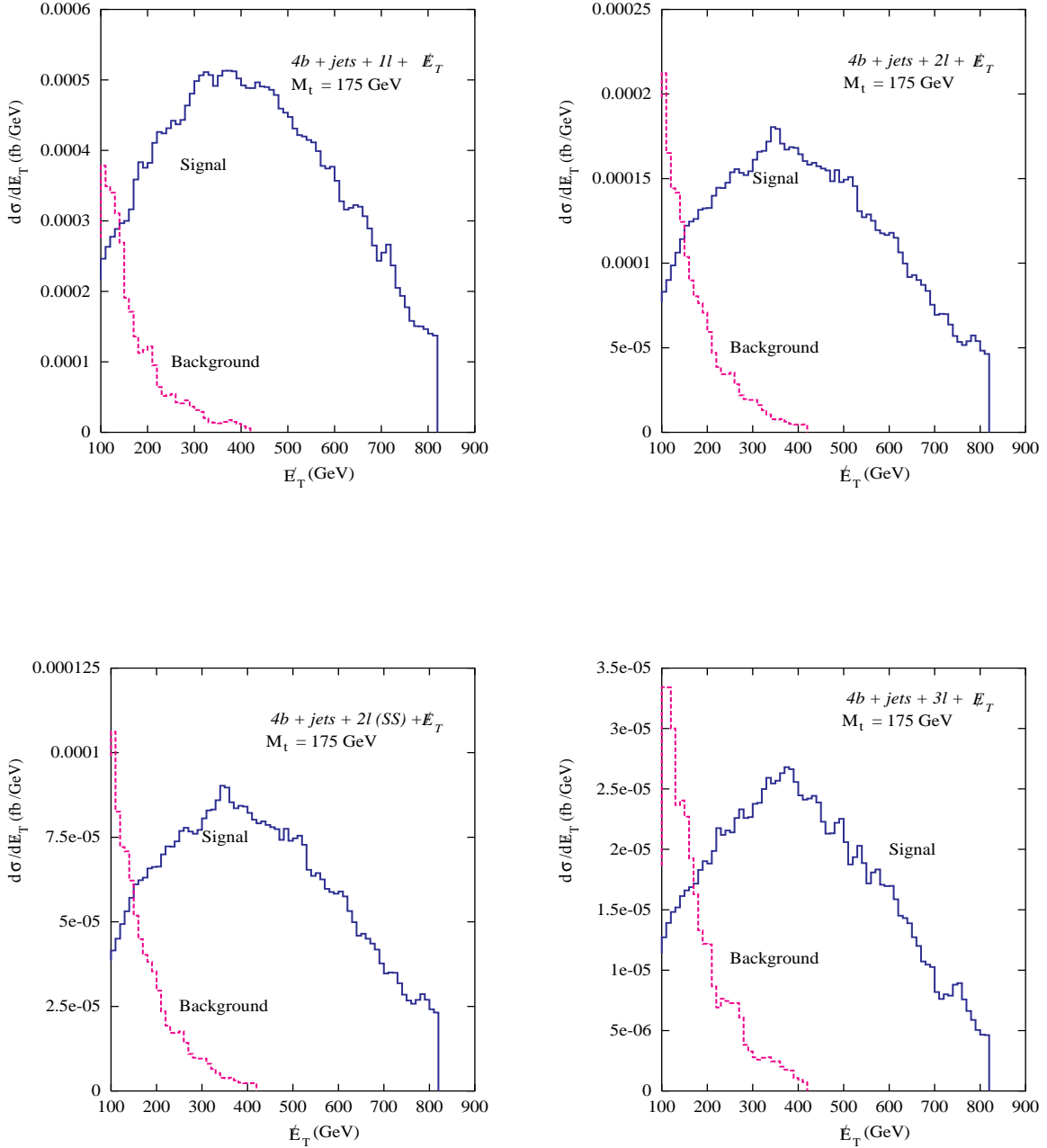


Fig. 8. Expected SUSY signal and the irreducible SM background from $t\bar{t}$ are shown in the single lepton, dilepton, same sign dilepton and trilepton channels with ≥ 3 b -tags for the focus point region ($m_0 = 2$ TeV, $M_{1/2} = 500$ GeV, $\tan\beta = 10$) [27].

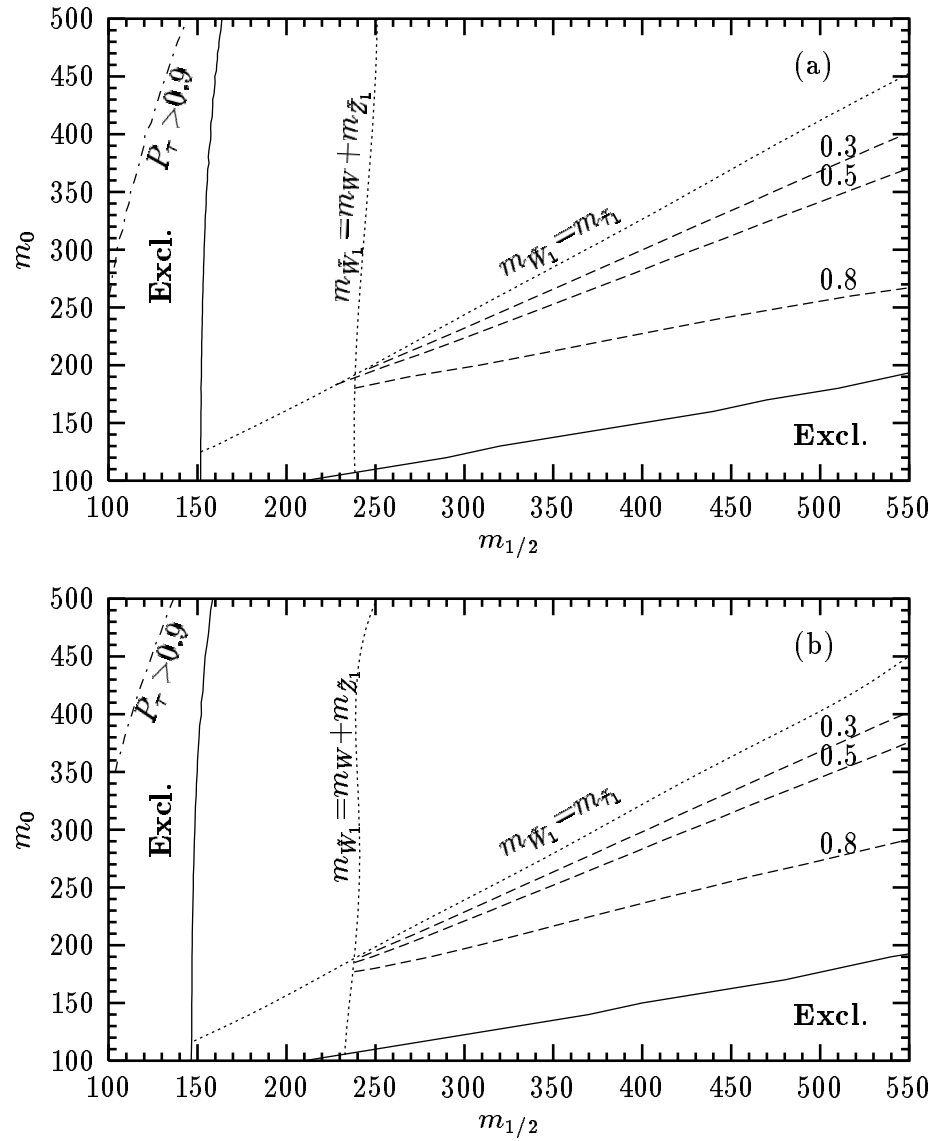


Fig. 9. $BR(\tilde{\chi}_1^\pm \rightarrow \tilde{\tau}_1 \rightarrow \tau \chi_1^0)$ is shown in the $m_0 - M_{1/2}$ plane for $A_0 = 0$, $\tan \beta = 30$ and (a) positive μ , (b) negative μ . The entire region to the right of the dot-dashed line corresponds to $P_\tau > 0.9$ [33].

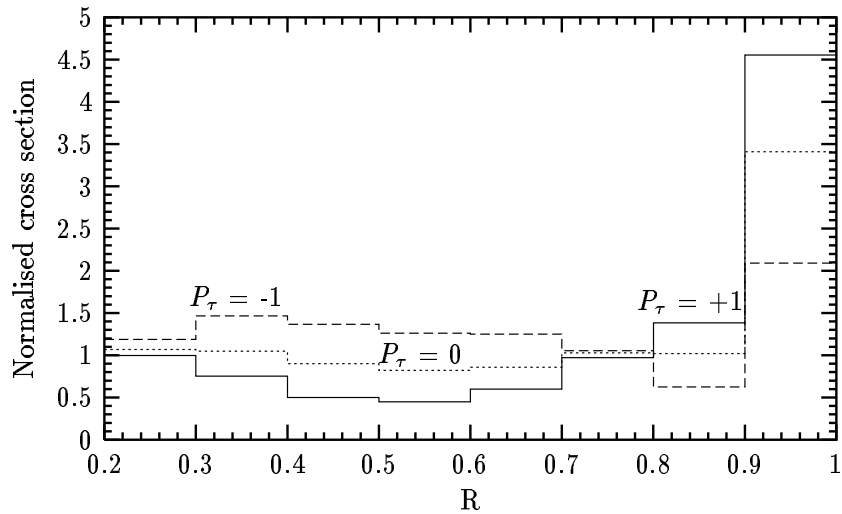


Fig. 10. The normalised SUSY signal cross-sections are shown for $P_\tau = 1$ (solid), 0 (dotted) and -1 (dashed) in the 1-prong hadronic τ -jet channel as functions of the τ -jet momentum fraction (R) carried by the charged prong [33].